GFDM-OQAM Performance Analysis Using Linear Equalization for Audio Transmission

Anggun Fitrian Isnawati *, Mas Aly Afandi, Khoirun Ni'amah, and Heru Adi Prasetyo

Institut Teknologi Telkom Purwokerto, Purwokerto 53147, Indonesia
Email: anggun@ittelkom-pwt.ac.id (A.F.I.); aly@ittelkom-pwt.ac.id (M.A.A.); khoirun@ittelkom-pwt.ac.id (K.N.);
heru@ittelkom-pwt.ac.id (H.A.P.)
*Corresponding author

Abstract—In order to minimize Inter-Carrier Interference (ICI), Inter-Symbol Interference (ISI), and Out of Band (OOB) impacts on Orthogonal Frequency Division Multiplexing (OFDM) systems, strong wireless communication performance is required. The use of Generalized Frequency Division Multiplexing (GFDM) is based on the requirement for a block-based multi-carrier technology in which each subcarrier is generated with a filter in the form of non-rectangular pulses known as pulse shaping. Meanwhile, Offset QAM (OQAM) is used to achieve better spectral efficiency than QAM and simultaneously reduce the occurrence of ICI and ISI. In this study, the effect of adjusting the roll-off factor value on the pulse shaping filter utilized is examined in order to detect the original signal supplied by the transmitter using two linear equalizations: Zero Forcing (ZF) and Minimum Mean Square Error (MMSE). The results show that the Signal to Noise Ratio (SNR) used in this study is varied from 0 dB to 15 dB, and the Bit Error Rate (BER) obtained when the SNR is 15 dB on GFDM-OQAM using ZF and MMSE are 0.03872 and 0.01986 respectively. Then this study indicates that the GFDM-OQAM system using MMSE equalization has a better BER value than the GFDM-OQAM system using ZF equalization. In addition, the greater the use of the roll-off factor, the lower the performance of the BER system because there is a greater excess bandwidth which is linear with the magnitude of the roll-off factor.

Keywords—Generalized Frequency Division Multiplexing (GFDM), offset QAM, Minimum Mean Square Error (MMSE), pulse shaping, roll-off factor, zero forcing

I. INTRODUCTION

The demand for higher data rates and lower latency, over the past decade has driven the rapid development of mobile and wireless communication systems [1]. One of them is the discovery of the multi-carrier modulation technique known as Orthogonal Frequency Division Multiplexing (OFDM), which is unquestionably used as the primary technology in radio communication networks. OFDM has the advantages of high spectral efficiency and immunity to multipath fading. But behind these advantages, OFDM has disadvantages such as Peak Average Power Ratio (PAPR) values, out of band (OOB) radiation and Inter-Carrier-Interference (ICI). Thus, OFDM cannot be able to satisfy the requirements of high-performance systems in the future [2].

A flexible multicarrier modulation scheme named Generalized Frequency Division Multiplexing (GFDM) has been proposed for the air interface of future cellular networks (5G) [3]. GFDM is a block-based multi-carrier technique that overcomes the shortcomings of OFDM by forming each subcarrier with a non-rectangular pulse filter known as pulse shaping [2]. Because of its flexibility and advantage over OFDM due to its orthogonality, GFDM is the technology best suited for 5G [4], as well as UFMC and Filter Bank Multi Carrier (FBMC) [5] and also Windowed Cyclic Prefix Circular OQAM (WCP-COQAM) [6, 7].

Quadrature Amplitude Modulation (QAM) is a common type of digital modulation used in transmission systems. However, there are disadvantages to QAM modulation, including the difficulty of symbol determination and Inter-Carrier Interference (ICI) [8]. Inter-symbol interference (ISI) and inter-carrier interference (ICI) are possible with GFDM due to its non-orthogonal characteristics. As a result, it is believed that QAM is insufficient for use in GFDM modulation [9]. To overcome this problem, it is necessary to Utilize Offset QAM (OQAM) modulation [2]. This condition will produce better spectral efficiency and at the same time reduce the occurrence of ICI and ISI. OQAM modulation on GFDM performs better than QAM modulation [2, 10].

Equalization is the process of providing an inverse estimate of the channel response using a linear filter. Zero Forcing (ZF) and Minimum Mean Square Error (MMSE) equalization types, which are linear equalizations, have been widely used in previous communications system, including OFDM [11–16], and FBMC [17]. These two equalizations have also been widely implemented in several studies related to GFDM [18–20]. The ZF is the most commonly used type of equalization or symbol detection algorithm due to its simple concept [21]. Additionally, ZF equalization is employed at the receiver to eliminate the ISI and ICI. MMSE equalization describes an approach to minimizing the value of the Mean Square Error (MSE), which is a common measure for quality

measurements. The major characteristic of the MMSE equalization is that it reduces the output's total noise power and ISI component, although without totally eliminating the ISI. MMSE equalization has better performance than Zero Forcing because it not only suppresses ISI but also minimizes noise power [13, 22]. The ideal use of a forming filter, namely raised cosine or root raised cosine, is commonly used in GFDM systems. By combining GFDM technique and modulation index [23] as well as the use of a pulse shaping filter, the GFDM system is very suitable for 5G scenarios [24]. The use of ZF and MMSE equalization is also carried out on the GFDM-OQAM system using MIMO Spatial Multiplexing for bit data transmission [25].

This paper reviews the performance of GFDM-OQAM using linear equalization in audio data transmission. The parameters used to analyze the performance of GFDM use Signal to Noise Ratio (SNR) and Bit Error Rate (BER) parameters using Zero Forcing (ZF) and Minimum Mean Square Error (MMSE) equalization. It also examined the impact of changes in the roll-off factor on the application of pulse shaping in GFDM.

The remainder of this work is divided into five sections. Section I provides an Introduction, and Section II explains the research method, which includes the proposed GFDM-OQAM transceiver, GFDM-OQAM modem, and simulation parameters. Section III examines GFDM-OQAM utilizing linear equalization, whereas Section IV contains the results and discussion session. We offered our conclusions at the end of this study.

II. RESEARCH METHOD

The GFDM-OQAM transceiver block diagram can be explained in Fig. 1 below.

Fig. 1 shows the modeling of the GFDM system that uses 16-QAM modulation using audio transmission data that is converted into a binary source form and will produce output in the form of audio transmission data. In this study, the input data used is in the form of audio files

with the provisions that the file format is .wav. The audio signal must first be converted into a stream of binary data before it can be transmitted. The normalized amplitude value of the audio signal ranges from −1 Volt to +1 Volt. The audio signal is converted to binary form, so that it can be transmitted.
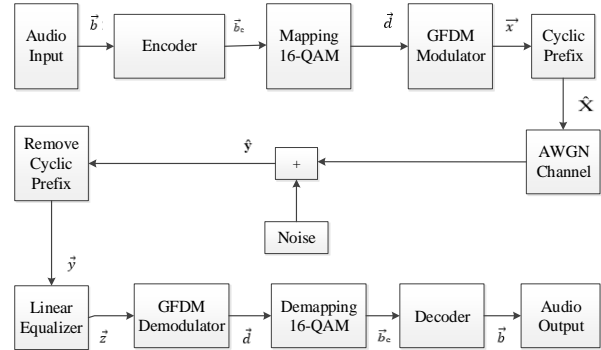

Fig. 1. The Block Diagram of GFDM-OQAM Transceiver.

The pulse shaping type used in GFDM is a Root-Raised Cosine (RRC) filter [26] with a roll-off factor variation of 0.3; 0.5; and 1. Then $v(t) = t^2(35 - 84t + 70t^2 - 20t^3)$ is a Meyer auxiliary function with a defining range $0 < \alpha < 1$. After obtaining the RRC pulse from the equation used, pulse g[n] shifted circularly in the time and frequency domains to produce a pulse shaping. To increase the bandwidth efficiency, the RRC pulse shaping is used.

Figs. 2−3 show the block diagrams of the GFDM-OQAM modulator and the GFDM-OQAM demodulator. GFDM is a block based non-orthogonal multicarrier technique where the complex valued data symbols are grouped in the time-frequency lattice into one 100 block. Each block consists of a total number of K sub-carriers and M symbols as depicted in [26]. To put it simply, the data are up-sampled first, then pulse-shaped using a prototype filter function. This makes use of the tail biting idea offered by the modulo operation-based circular convolution. The final step is up-conversion to the associated subcarrier frequency.
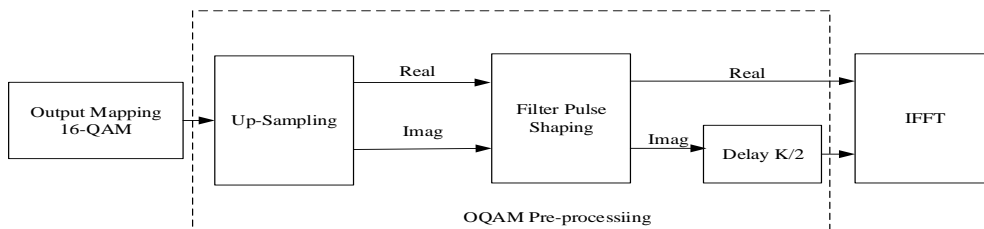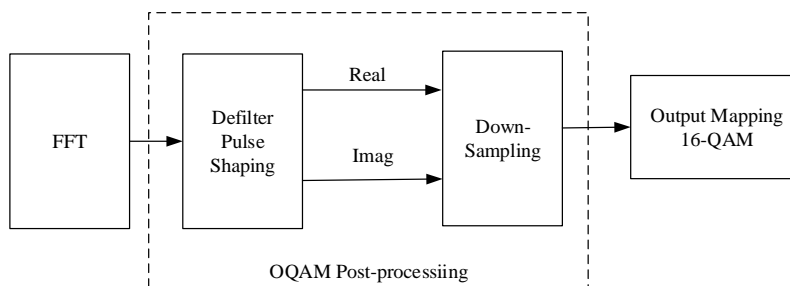

Fig. 2. The GFDM-OQAM modulator.

Fig. 3. The GFDM-OQAM demodulator.

The simulation parameters utilized in this study are listed in Table I below:

TABLE I. SIMULATION PARAMETERS

No	Parameter	Notation	Value
1	Modulation type	M	16-QAM
2	Audio data input	-	90 seconds
3	Pulse shape filter	g	Root raised cosine
4	Roll-off factor	α	{0.3; 0.5; 1}
5	Channel model	n(t)	AWGN

III. GFDM-OQAM USING LINEAR EQUALIZATION

A. GFDM-OQAM

1) The concept of GFDM-OQAM

GFDM is a non-orthogonal based multi-carrier technique, consisting of K subcarriers and M symbols in each block. GFDM-OQAM modulation uses the same components as GFDM with two main differences. The first difference is using QAM mapping, followed by applying M/2 sample offsets in the time domain between the in-phase and quadrature components of complex QAM data. The resulting OQAM mapping allows efficient reduction of both ICI and ISI when properly designed filters are applied. The second difference is that the orthogonality of the pulse shape can be achieved without the need for cyclic prefixes, which in turn increases the spectral efficiency.

The GFDM-OQAM system uses pulse shaping root raised cosine, and the orthogonality of a waveform can be obtained by transmitting $d_{k,m}^{[i]}$ and $d_{k,m}^{[q]}$, respectively shows the real and imaginary parts of $d_{k,m}$ using real value, filter $g_{k,m}[n]$ with offset M/2, phase rotation π/2 radian between sub-carriers and sub-symbols. Mathematically, the signal sent by the GFDM system using OQAM can be written as the following equation [9]:

$$x[n] = \sum_{k=0}^{K-1}\sum_{m=0}^{M-1} d_{k,m}^{(i)} g_{k,m}^{(i)}[n] + \sum_{k=0}^{K-1}\sum_{m=0}^{M-1} d_{k,m}^{(q)} g_{k,m}^{(q)}[n] \tag{1}$$

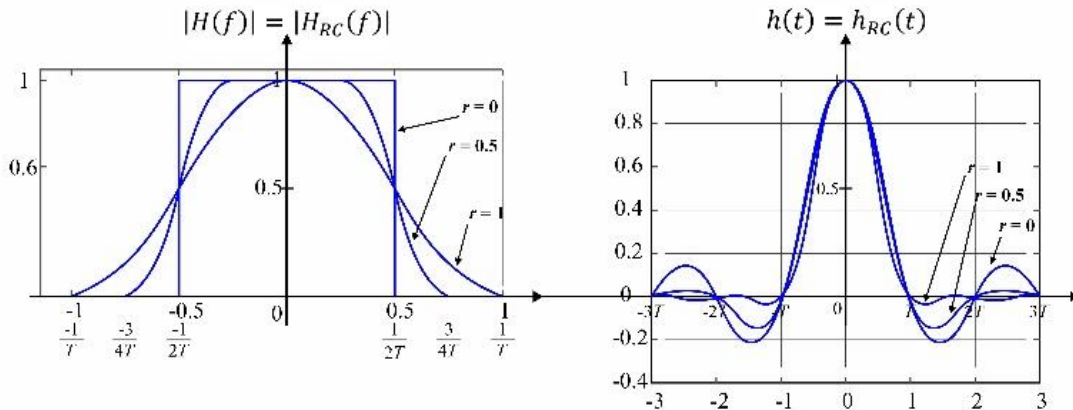This equation can be used to rewrite the transmitted GFDM signal [9]:

$$x = \boldsymbol{A}^{(i)}\boldsymbol{d}^{(i)} + \boldsymbol{A}^{(q)}\boldsymbol{d}^{(q)} \tag{2}$$

Based on Eq. (2), column matrix A$^{(i)}$ and A$^{(q)}$ sequentially related into $g_{k,m}^{(i)}$ and $g_{k,m}^{(q)}$ [24].

2) Pulse shaping and roll-off factor

One of the methods for controlling ISI is to properly shape the transmitted pulses. In order to eliminate ISI and ICI that are introduced by pulse shaping filters, interference cancellation techniques are used [27]. The filter employed in the pulse shaping process needs to adhere to the Nyquist criteria [28]:

$$h_{eff}(t) = \frac{\sin\left(\frac{\pi t}{T_s}\right)}{\pi t}.z(t) \tag{3}$$

It is assumed that the distortion in the transmission channel can be eliminated by an equalizer which has the same transfer function as the inverse of the channel response, then the transfer function h$_{eff}$ (f) can be selected as a result of multiplying the transfer function of the filters on the transmitter and receiver sides. The transfer function h$_{eff}$ (f) can be obtained by placing the value of the transfer function h$_{eff}$ (f) in each filter on the transmitter and receiver. For the system to have a matching filter response that can reduce bandwidth and ISI.

Before being transmitted, the signal undergoes a pulse shaping filter Root-Raised Cosine (RRC) process by convoluting the symbol with the response impulse filter. The impulse response of the Root-Raised Cosine (RRC) filter can be seen in the following Eq. (4).

$$h(t) = \frac{\sin\left(\pi\frac{t}{T}(1-\alpha)\right)+4\alpha\frac{t}{T}\cos\left(\pi\frac{t}{T}(1+\alpha)\right)}{\pi\frac{t}{T}\left(1-(4\alpha\frac{t}{T})^2\right)} \tag{4}$$

Roll-off factor (α) has a range of values from 0 to 1 and controls the amount of out of band signal. With a value of α=0, the filter is an ideal filter that suppresses all Out of Band (OOB) signals. In the time domain, the side lobes of the impulse filter response increase as the roll-off factor are decreased. This causes an increase in the peak power of the transmitted signal after pulse shaping.

Fig. 4. Raised cosine in the frequency domain and time domain [29, 30].

According to the Fig. 4, a digital signal with a higher cosine characteristic occupies a bandwidth that spans from $fb=1/(2Ts)$ Hz (α=0) to $fb=1/(Ts)$ Hz (α=1). In the frequency domain, for the condition $\alpha = 0$, the resulting spectrum is rectangular which is identical to the shape of an ideal filter. Whereas in the time domain it is a sinc signal which has zero crossing at $t = T, 2T, ..., nT$.

3) Offset quadrature amplitude modulation (OQAM)

This study uses 16-QAM modulation, in which one symbol contains 4 bits of data to be transmitted. Symbol can represent 16 different values (0000, 0001, 0010……1111). Each symbol consists of quadrature phase (Q) and in-phase (I) components. The 16-QAM modulation constellation diagram can be shown in the Fig. 5 [31].
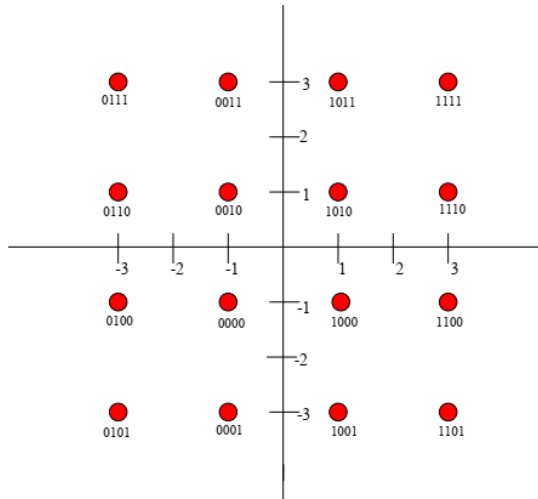
Fig. 5. 16-QAM constellation [31].

In GFDM systems, the quadrature phase (Q) component of the symbols is moved by M/2 in 16-OQAM as opposed to 16-QAM. Shifted quadrature seeks to keep symbol energy from transferring to any other places in the constellation of symbols. Furthermore, changing the GFDM symbols' quadrature phase component causes transitions between the in phase (I) and quadrature phase (Q) components to occur non-concurrently. OQAM should avoid inter-carrier interference (ICI) with the help of these goals. Afterwards, the GFDM modulator will handle the symbol stream coming from the system with the QAM mapper or the system with the OQAM mapper [32]. The constellation diagram of QAM and OQAM symbols is shown in Fig. 6 below [33].

Compared to QAM mapping, OQAM mapping performs significantly better while having little alterations to the transmitting symbols. OQAM mapping has a small-but-very-important changes when compared to QAM mapping. In OQAM, the Q component is shifted by half the symbol rate. In OQAM modulation, the phase shift occurs is limited to 0° and ± 90° every T second, unlike in QAM which occurs a phase jump of up to 180°. In OQAM mapping, the I and Q components do not have a transition at the same time. This demonstrates that the OQAM

transition never exceeds 90°. The output of the modulator, $x(m)$, is as follows [34].

$$x(m) = \sum_{k=0}^{\infty} \sum_{n=0}^{N-1} [a_{k,n}h(m-kN) + jb_{k,n}h\left(m - kN + \frac{N}{2}\right)]e^{j\left(\frac{2\pi}{N}m+\frac{\pi}{2}\right)n} \quad (5)$$

From the equation above will be obtained:

$$C_{k,n} = a_{k,n} + jb_{k,n} \quad (6)$$

A block diagram of the OQAM modulator using pulse shaping is shown in Fig. 7. Each channel consisting of real part ($a_{k,n}$) and imaginary part ($b_{k,n}$) is symbolized by $C_{k,n}$, then filtered with pulse shaping $h(m)$ and $h(m + N/2)$. $C_{k,n}$ is the complex data transmitted on the n_{th} subcarrier and k_{th} sub symbol. The two parts are added together and shifted at a predetermined frequency using baseband modulation.
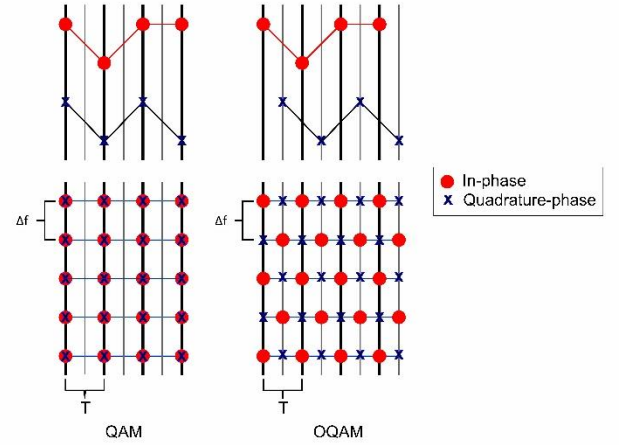

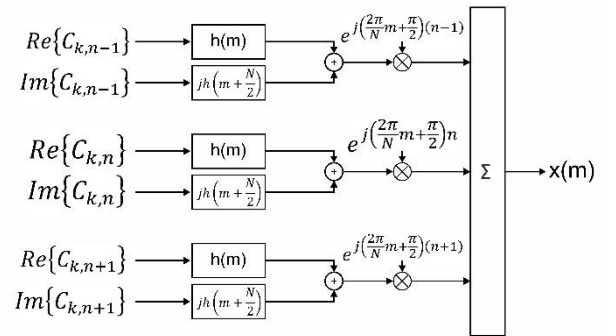Fig. 6. The constellation diagram of QAM and OQAM symbols [33].

Fig. 7. The OQAM modulator using pulse shaping [35].

A block diagram of the OQAM demodulator using pulse shaping is shown in Fig. 8. The received signal is then baseband modulated on each channel to shift it back to its initial state, and it is then re-filtered to separate the real and imaginary components, yielding one sample per symbol. The real part of the signal can be written as follows [36]:

$$a_{k,n} = Re\left\{\sum_m h(m)x(kN-m)e^{j\left(\frac{2\pi}{N}m-\frac{\pi}{2}\right)n}\right\} \quad (7)$$

while the imaginary part of the signal is written as follows [36]:

$$b_{k,n} = Im\left\{\sum_m h\left(m - \frac{N}{2}\right)x(kN - m)e^{j\left(\frac{2\pi}{N}m - \frac{\pi}{2}\right)n}\right\} \quad (8)$$
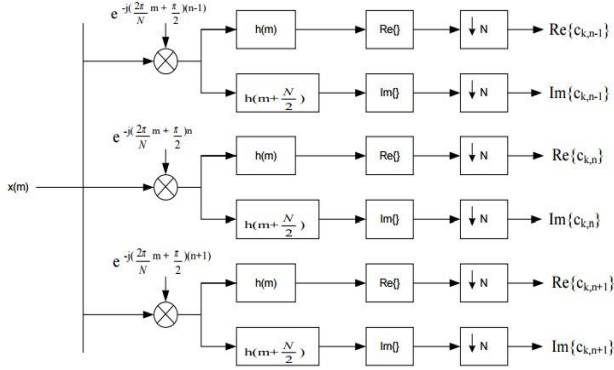

Fig. 8. The OQAM demodulator using pulse shaping [35].

4) Linear equalization

Let y be a vector containing y[n] time samples at the receiver, after the signal has passed through the AWGN channel. In this case $y = x + n$, where n ~ $(0, \sigma_n^2)$ is the noise vector containing the AWGN. The first way to receive a GFDM signal is formed by finding the $\mathbf{A}^+$ matrix, where $\mathbf{A}^+\mathbf{A}=\mathbf{I}$, and I is identity matrix of the appropriate size. Depends on the level $\mathbf{A}$, can be calculated as $\mathbf{A}^+ = (\mathbf{A}^H\mathbf{A})^{-1}\mathbf{A}^H$ or $\mathbf{A}^+ = \mathbf{A}^H(\mathbf{A}\mathbf{A}^H)^{-1}$. Then the equation for the Zero Forcing (ZF) receiver is obtained as in the following equation [4, 37]:

$$d_{ZF} = \mathbf{A}^+\mathbf{y} \quad (9)$$

Besides ZF, the second way to obtain GFDM signals is to apply a matched filter (MF) $\mathbf{A}^H$ to the receiver. The equation can be written as follows [4, 37]:

$$d_{MF} = \mathbf{A}^H\mathbf{y} \quad (10)$$

The third method is linear minimum mean square error (MMSE), which can be written as the following equation [4, 37]:

$$d_{MMSE} = \mathbf{A}^+\mathbf{y} \text{ with } \mathbf{A}^+ = \left(\frac{\sigma_n^2}{\sigma_n^2}\mathbf{I} + \mathbf{A}^H\mathbf{A}\right)^{-1}\mathbf{A}^H \quad (11)$$

MMSE is used to overcome the noise gain of the ZF receiver by balancing the variance of the noise and symbol data σ_d^2 [35].

IV. SIMULATION RESULTS

The simulation output included a comparison of SNR vs. BER for GFDM-OQAM, BER performance for GFDM-OQAM systems with and without ZF and MMSE equalization, and a comparison of GFDM-OQAM ZF and MMSE on roll-off factor variation.

A. Data Transmission

In this simulation, audio files were utilized as the input data, and Fig. 9 depicts the digital audio signal, which has a common sampling frequency of 44,100 Hz (44.1 kHz),

or around 2.268x10⁻⁵ seconds or 0.02268 milliseconds of sampling time. A point must have amplitude 1 added in order to the conversion to a binary number to be positive. This makes it possible for the audio signal to be transmitted to the receiver.
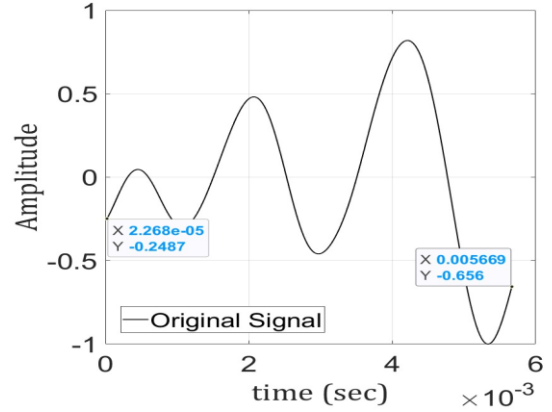

Fig. 9. Transmitted data.

B. GFDM-QAM and GFDM-OQAM System Using Linear Equalization

It is required to apply equalization on the receiving end to improve system performance. In this system, the linear equalization techniques used are Zero Forcing (ZF) and Minimum Mean Square Error (MMSE).

The GFDM-QAM and GFDM-OQAM communication system using Zero Forcing equalization based on BER performance are shown in figures below. Figs. 11−13 as follows are the performance comparison of the Theory 16-QAM, the simulation results of the GFDM-QAM and the GFDM-OQAM using ZF equalization.

In Figs. 10−11, the simulation result of Theory 16-QAM showed that when the SNR is 0 dB, the resultant BER is 0.1852. When the SNR is 15 dB, the resulting BER is 0.004445. The comparison results of SNR to BER in Fig. 10 showed that the performance comparison between the Theory 16-QAM and the GFDM-QAM using ZF equalization, meanwhile Fig. 12 described the performance comparison between the Theory 16-QAM and the GFDM-OQAM system using ZF equalization.
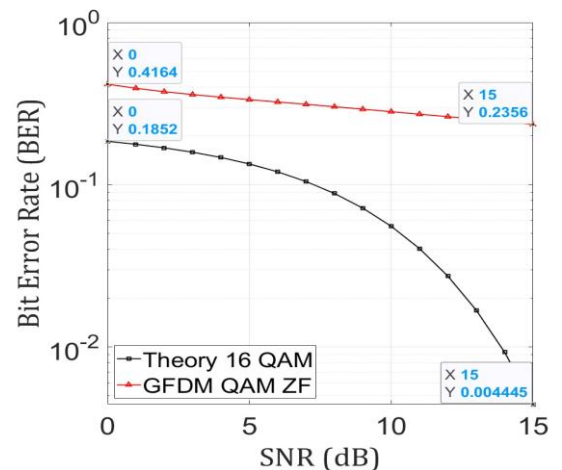

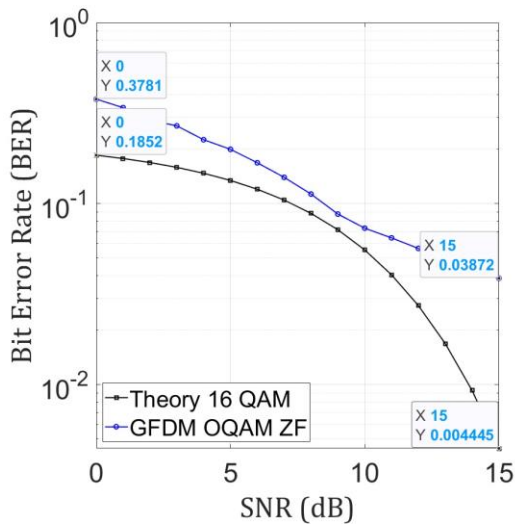Fig. 10. Performance comparison of theory 16-qam and Gfdm-Qam using ZF equalization.

Fig. 11. Performance comparison of theory 16-QAM and GFDM-OQAM using ZF equalization.

However, the BER simulation results have demonstrated that the performance of both, the GFDM-QAM and the GFDM-OQAM system using ZF, have improved in the ensuing BER alterations. The following Fig. 12 illustrates it. As shown in this figure, performance of the GFDM-OQAM system using ZF is superior to the GFDM-QAM system using ZF.
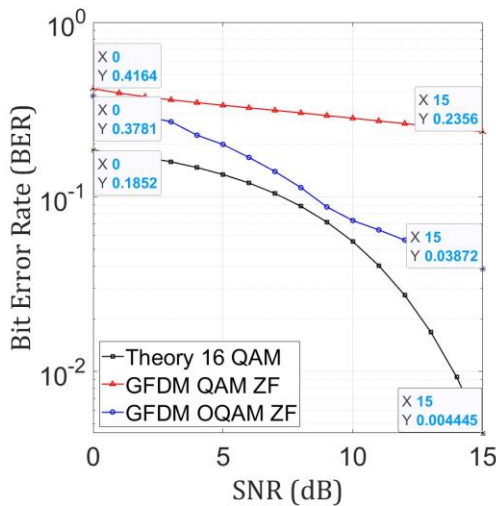

Fig. 12. Performance comparison of theory 16-QAM, GFDM-QAM and GFDM-OQAM using ZF equalization.

Fig. 12 showed that the simulation of BER value generated by GFDM QAM and GFDM-OQAM when the SNR is 0 dB, the resulting BER are 0.4164 and 0.3781 respectively. Meanwhile, when the SNR value is 15 dB, the resulting BER are 0.2356 and 0.03872 respectively. There is a significant reduction in BER results, though it is not as good as the 16-QAM theory that has received BER 0.1852 in SNR 0 dB and 0.004445 in SNR 15 dB. This occurs as a result of the use of the AWGN channel, which already contains noise. As a result, because the received signal already contains a lot of noise, increasing the SNR value has the effect on BER.

Based on those three figures, it can be concluded that the use of OQAM is superior to QAM, and the use of ZF equalization is able to provide even better performance than without ZF equalization.

C. GFDM-QAM and GFDM-OQAM System Using MMSE Equalization

Similar to how ZF equalization is applied, MMSE equalization is applied on the receiving side to enhance system performance. Figs. 13−14 below illustrates the use of MMSE equalization, both in GFDM-QAM and GFDM-OQAM. To demonstrate how the BER performances are improving in those conditions while the BER values are decreasing from 0.4373 in SNR 0 dB to 0.2456 in SNR 15 dB for GFDM-QAM performance and decreasing from 0.4059 in SNR 0 dB to 0.01986 in SNR 15 dB for GFDM-OQAM performance. Fig. 16 compares the BER performance of Theory 16-QAM, GFDM QAM and GFDM-OQAM Using MMSE Equalization. It may be inferred that using OQAM is better than using QAM and using MMSE equalization can provide greater performance than the system without MMSE equalization.
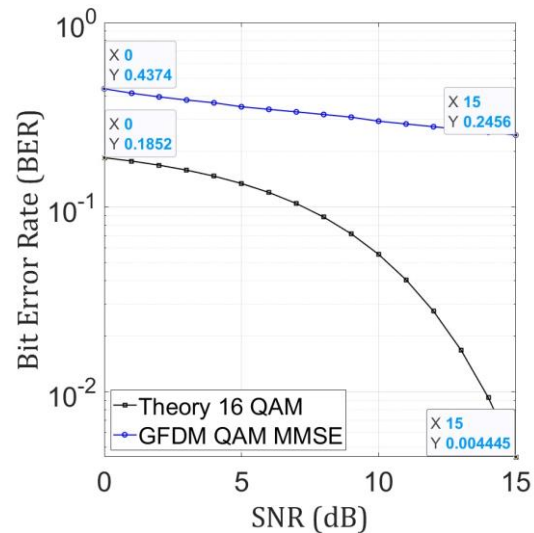

Fig. 13. Performance comparison of theory 16-QAM and GFDM-QAM using MMSE equalization.
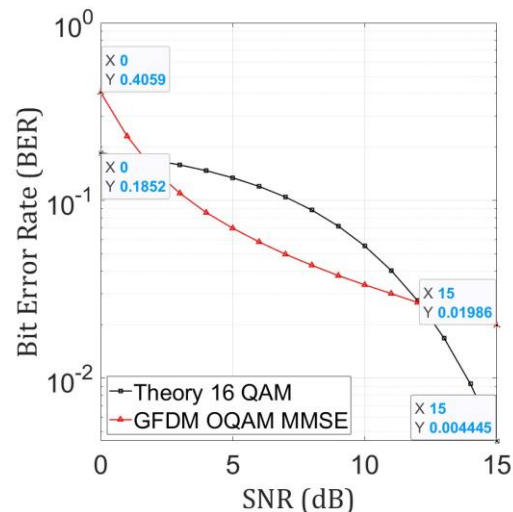

Fig. 14. Performance comparison of theory 16-QAM and GFDM-OQAM using MMSE equalization.
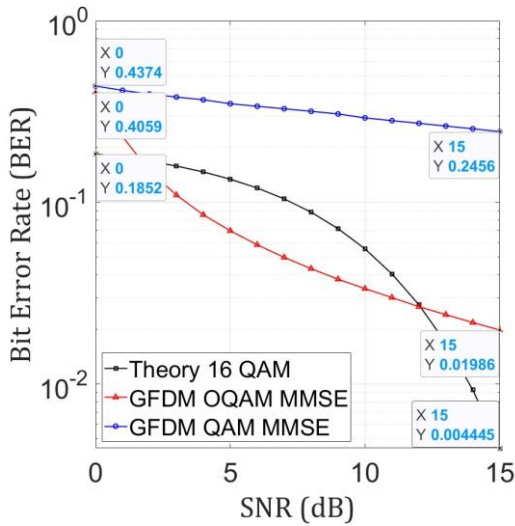
Fig. 15. BER comparison of theory 16-QAM, GFDM QAM vs GFDM-OQAM using MMSE equalization.
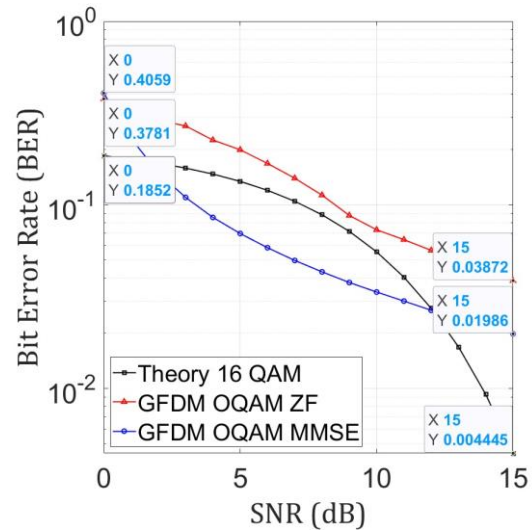

Fig. 17. BER comparison of GFDM-OQAM using ZF and MMSE equalization.

D. GFDM System Comparison using ZF and MMSE Equalization

The performance comparison of the ZF and MMSE equalization used in both the GFDM-QAM and GFDM-OQAM systems, which uses linear equalization, will be covered in this discussion. When equalizer ZF and MMSE are used, Fig. 16 shows how the GFDM-QAM performs for BER comparison. The results demonstrate that the BER results of the GFDM-QAM system utilizing ZF equalization and MMSE equalization are 0.2456 and 0.2356, respectively, while Fig. 18 exhibits the functionality of GFDM-OQAM for comparison of BER when using ZF and MMSE equalization. According to the findings, the ZF and MMSE results for BER on the GFDM-OQAM system are, respectively, 0.03872 and 0.01986.

It can be seen from the graph in Figs. 16–17 that both GFDM-QAM and GFDM-OQAM systems that employing MMSE equalization show better performances in terms of BER, than both the systems that using ZF equalization.
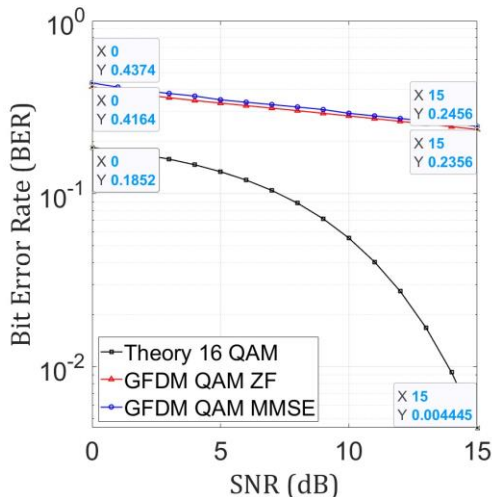
E. GFDM-OQAM System Based-on Roll-off Factor Variation

GFDM-OQAM graphs using ZF and MMSE equalizations and variations in the roll-off factors for the pulse shaping filter used is shown respectively in the next Figs. 18–19.

Figs. 18–19 provide an explanation of how the GFDM-OQAM system's performance is impacted by the employment of the roll-off factor in the pulse shaping filter.

Fig. 18 shows the effect of changing the roll-off factor on the GFDM-OQAM ZF system. It can be seen from the figure that when $\alpha = 1$, BER value of 0.07372 is obtained at an SNR of 15 dB. This value is greater than the BER value when α is 0.5 and 0.3 which is 0.06342 and 0.05342 at the same SNR of 15 dB.

Fig. 16. BER comparison of GFDM-QAM using ZF and MMSE equalization.
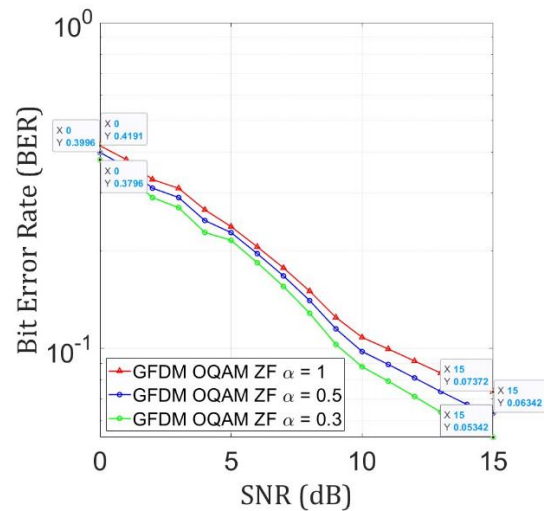

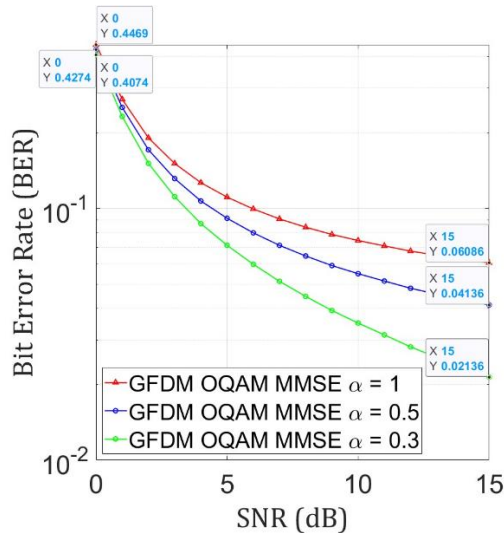Fig. 18. GFDM-OQAM ZF using variations of roll-off factor.

Fig. 19. GFDM-OQAM MMSE using variations of roll-off factor.

The effect of adjusting the roll-off factor on the GFDM-OQAM MMSE system is shown in Fig. 20. The figure shows that when α = 1, BER value of 0.06086 is produced at an SNR of 15 dB. At the same SNR of 15 dB, this number is greater than the BER value when α are 0.5 and 0.3, which are 0.04136 and 0.02136. Or in other words, the BER performance will be better (having a smaller BER value) if a small roll-off factor value is used.

Generally, through several simulation results it can be shown that the effect of the roll-off factor on BER performance is that the smaller the roll-off factor value, the smaller the BER value, which means the better the performance. Increasing the roll-off factor will also increase the excess bandwidth. In this scenario, lower system performance the higher the roll-off factor employed since the excess bandwidth will arise. An increase in the BER value induced by an increase in the roll-off factor value indicates a deterioration in system performance.

Applying OQAM mapping rather than QAM to the GFDM system is more successful. Benefits of GFDM-OQAM include its ability to satisfy application needs with high data rates and ICI-free, making it appropriate for 5G communication. According to the overall findings of this study, the GFDM-OQAM system using MMSE equalization with a small roll-off factor of 0.3 offers the best performance of all the possible outcomes.

V. CONCLUSION

Based on the simulation results, it can be said that using Offset-QAM mapping in GFDM system can deliver performance that is superior to QAM mapping, making GFDM-OQAM perform better than GFDM-QAM. Additionally, selecting the appropriate equalization can enhance system performance. It is evident from the two equalizations employed that MMSE equalization performs better than ZF equalization. The roll-off factor utilized can change in value, and as a result, the higher the roll-off factor, the higher the BER value obtained, or in other words, the lower the performance.

REFERENCES

[1] S. K. Bandari, V. V. Mani, and A. Drosopoulos, "Performance analysis of GFDM in various fading channels," *COMPEL: The International Journal for Computation and Mathematics in Electrical and Electronic Engineering*, vol. 35, no. 1, pp. 225–244, Jan. 2016.
[2] S. K. Bandari, V. V. Mani, and A. Drosopoulos, "OQAM implementation of GFDM," in *Proc. 2016 23rd International Conference on Telecommunications (ICT)*, Thessaloniki, Greece: IEEE, May 2016, pp. 1–5.
[3] S. K. Antapurkar, A. Pandey, and K. K. Gupta, "GFDM performance in terms of BER, PAPR and OOB and comparison to OFDM system," presented at the Advancement in Science and Technology, Rajasthan, India, 2016, p. 020039.
[4] M. Sameen *et al.*, "Comparative analysis of OFDM and GFDM," *Int J Adv Comput Tech Appl*., vol. 4, no. 2, p. 8, 2016.
[5] O. E. Ijiga, O. O. Ogundile, A. D. Familua, and D. J. J. Versfeld, "Review of channel estimation for candidate waveforms of next generation networks," *Electronics*, vol. 8, no. 9, p. 956, Aug. 2019.
[6] A. Lizeaga, P. M. Rodríguez, I. Val, and M. Mendicute, "Evaluation of 5G modulation candidates WCP-COQAM, GFDM-OQAM, and FBMC-OQAM in low-band highly dispersive wireless channels," *Journal of Computer Networks and Communications*, vol. 2017, pp. 1–11, 2017.
[7] A. Lizeaga, M. Mendicute, P. M. Rodriguez, and I. Val, "Evaluation of WCP-COQAM, GFDM-OQAM and FBMC-OQAM for industrial wireless communications with Cognitive Radio," in *Proc. 2017 IEEE International Workshop of Electronics, Control, Measurement, Signals and their Application to Mechatronics (ECMSM)*, Donostia, San Sebastian, Spain: IEEE, May 2017, pp. 1–6.
[8] K. Anish Pon Yamini, S. V. Akhila, K. Suthendran, and K. Srujan Raju, "Analysis of channel estimation in GFDM system," in *Proc. Data Engineering and Communication Technology*, vol. 63. Singapore: Springer Singapore, 2021, pp. 679–687.
[9] I. Gaspar, M. Matthe, N. Michailow, L. Leonel Mendes, D. Zhang, and G. Fettweis, "Frequency-shift offset-QAM for GFDM," *IEEE Commun. Lett.*, vol. 19, no. 8, pp. 1454–1457, Aug. 2015.
[10] S. K. Bandari, V. V. Mani, and A. Drosopoulos, "GFDM/OQAM implementation under Rician fading channel," in *Proc. 2016 International Conference on Advances in Computing, Communications and Informatics (ICACCI)*, Sep. 2016, pp. 256–260.
[11] F. Wang, "Pilot-based channel estimation in OFDM system," The University of Toledo, Ohio, 2011.
[12] F. C. Vilar, "Implementation of zero forcing and MMSE equalization techniques in OFDM," University of Fortaleza, Brazil, 2014.
[13] H. Wang and R. Song, "MMSE precoding with configurable sizes for GFDM systems," in *Proc. 2017 9th International Conference on Wireless Communications and Signal Processing (WCSP)*, Nanjing: IEEE, Oct. 2017, pp. 1–6.
[14] N. S. Kumar, "Performance analysis and comparison of zero – Forcing SIC and MMSE SIC for MIMO Receivers using BSPK and

16- QAM Modulation methods," *International Journal of Computer Science & Engineering Technology*, vol. 1, no. 8, p. 4, 2011.

[15] P. S. Sidhu, G. Singh, and A. Grover, "An analytical design: Performance comparison of MMSE," *Innov Syst Design Eng*., vol. 3, p. 16, 2012.

[16] D. V. Latha, N. Nandhini, A. Pavithra, A. Poornima, and I. S. Ancy, "BER Reduction using ZF-SIC and MMSE-SIC algorithm in LTE-a network," *International Journal of Pure and Applied Mathematics*, p. 9, 2018.

[17] A. F. Isnawati, V. O. Citra, and J. Hendry, "Performance analysis of audio data transmission on FBMC - Offset QAM system," in *Proc. 2019 IEEE International Conference on Industry 4.0, Artificial Intelligence, and Communications Technology (IAICT)*, BALI, Indonesia: IEEE, Jul. 2019, pp. 81–86.

[18] V. Lamani and D. P. G. Poddar, "Generalized frequency division multiplexing for 5G cellular systems: A tutorial paper," *AKGEC International Journal of Technology*, vol. 8, no. 1, p. 7, 2017.

[19] E. N. O. Herawati, A. F. Isnawati, and K. Ni'amah, "Analysis of GFDM-OQAM performance using zero forcing equalization," in *Proc. 2021 IEEE International Conference on Communication, Networks and Satellite (COMNETSAT)*, Purwokerto, Indonesia: IEEE, Jul. 2021, pp. 135–140.

[20] W. Indah Sari, A. F. Isnawati, and K. Ni'amah, "Performance analysis GFDM Using MMSE equalization in audio transmission," in *Proc. 2021 IEEE International Conference on Communication, Networks and Satellite (COMNETSAT)*, Purwokerto, Indonesia: IEEE, Jul. 2021, pp. 141–145.

[21] R. Hidayat, A. F. Isnawati, and B. Setiyanto, "Channel estimation in MIMO-OFDM spatial multiplexing using Least Square method," in *2011 International Symposium on Intelligent Signal Processing and Communications Systems (ISPACS)*, IEEE, 2011, pp. 1–5.

[22] J. Hendry and A. F. Isnawati, "Analisis perbandingan kinerja ekualisasi zero forcing dan MMSE pada FBMC-OQAM," *ELKOMIKA*, vol. 7, no. 3, p. 600, Sep. 2019.

[23] E. Ozturk, E. Basar, and H. A. Cirpan, "Generalized frequency division multiplexing with index modulation," in *Proc. 2016 IEEE Globecom Workshops (GC Wkshps)*, Washington, DC, USA: IEEE, Dec. 2016, pp. 1–6.

[24] Z. A. Sim, F. H. Juwono, R. Reine, Z. Zang, and L. Gopal, "Performance of GFDM systems using quadratic programming pulse shaping filter Design," *IEEE Access*, vol. 8, pp. 37134–37146, 2020.

[25] S. W. Tarbouche and A.-N. Assimi, "Performance of OQAM/GFDM in spatial multiplexing MIMO systems," *International Journal of Embedded and Real-Time Communication Systems*, vol. 11, no. 2, pp. 39–57, Apr. 2020.

[26] N. Michailow *et al.*, "Generalized frequency Division multiplexing for 5th generation cellular networks," *IEEE Trans. Commun.*, vol. 62, no. 9, pp. 3045–3061, Sep. 2014.

[27] N. Michailow, R. Datta, S. Krone, M. Lentmaier, and G. Fettweis, "Generalized frequency division multiplexing: A flexible multi-carrier modulation scheme for 5th generation cellular networks," presented at the German Microwave Conference (GeMiC), Ilmenau, Germany, 2012, p. 5.

[28] J. A. Yunas, A. Fahmi, and N. Andini, "Analisis reduksi papr dengan teknik clipping dan pulse shaping menggunakan filter RRC pada SC-FDMA," *eProceedings of Engineering*, vol. 3, no. 3, p. 8, Dec. 2016.

[29] Chethan, Ravisimha, and M. Z. Kurian, "The effects of Inter Symbol Interference (ISI) and FIR Pulse Shaping Filters: A survey," *International Journal of Advanced Research in Electrical, Electronics and Instrumentation Engineering*, vol. 3, no. 5, pp. 9411–9416, May 2014.

[30] H. M. Abdel-Atty, W. A. Raslan, and A. T. Khalil, "Evaluation and analysis of FBMC/OQAM systems based on pulse shaping filters," *IEEE Access*, vol. 8, pp. 55750–55772, 2020.

[31] R. Hdiji *et al.*, "IDROMel liverable 1.3.1, version 1.0 baseband functional specification Premilinary architecture," Bahria University, Pakistan, Jun. 2007.

[32] D. A. Feryando, T. Suryani, and Endroyono, "Performance analysis of regularized channel inversion precoding in multiuser MIMO-GFDM downlink systems," in *Proc. 2017 IEEE Asia Pacific Conference on Wireless and Mobile (APWiMob)*, Bandung: IEEE, Nov. 2017, pp. 101–105.

[33] A. F. Demir, M. Elkourdi, M. Ibrahim, and H. Arslan, "Waveform Design for 5G and Beyond," in *Proc. 5G Networks: Fundamental Requirements, Enabling Technologies, and Operations Management*, Hoboken, NJ, USA: John Wiley & Sons, Inc., 2018, pp. 51–76.

[34] V. Selvakumar, S. S. Nemalladinne, and P. Arumugam, "Analysis of LTE radio frame by eliminating cyclic prefix in OFDM and comparison of QAM and offset-QAM," Master Thesis, Linaeus University, Sweden, 2012.

[35] F. H. Ramadiansyah, "Perbaikan kinerja sistem generalized frequency division multiplexing dengan menggunakan offset quadrature amplitude modulation," Thesis, ITS, Surabaya, Indonesia, 2017.

[36] E. Wulansari, "Analisis kinerja teknik linear precoding Block diagonalization pada sistem multi user MIMO-GFDM menggunakan detektor MMSE," Master Thesis, ITS, Surabaya, Indonesia, 2018.

[37] F. Li, L. Zhao, K. Zheng, and J. Wang, "A interference-free transmission scheme for GFDM system," in *Proc. 2016 IEEE Globecom Workshops (GC Wkshps)*, Dec. 2016, pp. 1–6.